ARTICLE IN PRESS

X-ray dose detector based on color changing of light-emitting polymer–metal complex hybrid material

T. Schimitberger [a], G.R. Ferreira [a], M.F. Saraiva [b], A.G.C. Bianchi [a], R.F. Bianchi [a,*]

[a] Laboratory of Polymers and Electronic Properties of Materials, Department of Physics, Federal University of Ouro Preto, Ouro Preto – MG, 35400-000, Brazil
[b] Cancer Hospital of Muriae, Cristiano Varella Foundation, Muriaé – MG, 36880-000, Brazil

ARTICLE INFO

ABSTRACT

We report on the design, fabrication and performance of a poly (2-methoxy-5(2′-ethylhexyloxy)-p-phenylenevinylene)/tris-(8-hydroxyquinoline)aluminum (MEH-PPV/Alq$_3$) X-ray dose detector for improving safety for cancer patients shortly before radiation therapy. The detector consists of an inexpensive (<US$ 1) organic device that is irreversibly color changing from red, to yellow, to green and measures the delivered dose from the radiation beams of a linear accelerator (6 MV) in the range of 0–40 Gy. The effect of radiation on the optical properties of MEH-PPV/Alq$_3$ was described and we observed a strong correlation between the photoemission spectrum of Alq$_3$ and the photoemission and absorption spectra of MEH-PPV degraded by radiation. A series of tests was conducted on the performance of the organic detector in measuring depth-dose distribution of photon beams in a water phantom and demonstrating linearity in the shift of PL and absorption as functions of the dose. These results have enabled the qualitative and quantitative analysis of how the radiation instability of optical properties of MEH-PPV/Alq$_3$ can be used to develop an innovative organic device for radiation therapy.

1. Introduction

Radiation therapy has been used for several decades in the treatment of oncology patients, using radiation or particles to damage and destroy cancer cells [1]. It is shown that this field has undergone enormous progress over the last few decades and modern radiation therapies range from planning capacities to reduce patient set-up errors in clinical practices to standard dosimetric methodology for measuring single scan dose profiles and dose delivered to the tumor, as well as depth and cumulative dose, for the best possible therapy [2]. This proposed treatment aims to improve cancerous tumor control, thus reducing side and long-term effects of radiation therapy. The main radiation therapy modality is the external beam radiotherapy, or teletherapy treatment, in which the radiation source is placed outside the body and the emitted beam penetrates the tissues interacting with normal and cancerous cells [2–4]. Among the radiation oncology equipment available, some of the most popular for the treatment of deep seated tumors is the Linear Accelerator (LINAC), in which the external beam radiation therapy is delivered by means of high energy X-rays (6 MV) [5]. LINAC is the standard method for producing photons and electrons delivered to the tumor with extreme accuracy such as beam quality, direction, and intensity. It is programmed to send precise doses of radiation directly to cancer cells in a very targeted way through a state-of-the-art therapy called Intensity Modulated Radiation Therapy. The majority of tumors require doses in the range of 8–70 Gy, fractionated in doses of 1.8–2.0 Gy once a day, five times a week for 5–7 weeks.

We have performed an investigation of several studies on the impact of radiation on cancer treatments, which has been summarized in recent reviewed articles by Abdelaziz and Biggs [6,7]. Most of these works, however, aim to allow doctors to attack tumors more precisely, rather than identifying radiation injuries caused by software flaws and faulty programming on individual cases, which can be difficult to control due to LINAC's complexity [8]. These flaws have a serious impact on patient treatment, as seen in several reported treatment errors and incidents [8]. When these mistakes occur, they can be fatal; it is critical to prevent such errors in this extremely important field. Previous work by the American Association of Physicists in Medicine and the American Society of Radiation Oncology supports the view that "error reporting systems should be developed in radiation therapy" to "protect the safety of each and every patient" [8–11]. From this point of view, an easy-to-use, easy-to-read and low-cost dosimeter, that is also more accessible to people in places with limited resources, may ensure that every treatment will be as safe as possible. Hence it is an innovative proposal for the psychological comfort of cancer patients as it ensures proper functioning of LINACs. In this case, each patient will be able to personally monitor the response of the radiation detector shortly before being irradiated and

* Corresponding author. Tel.: +55 31 35591667; fax: +55 31 35591667.
E-mail address: bianchi@iceb.ufop.br (R.F. Bianchi).

therefore making sure that the prescribed dose for their cancer treatment will be administered properly, avoiding fatal radiation overdose or underdose caused by software problems and poor quality control for radiation delivery in many hospitals. Concomitantly, a notable advance in the development of personal dosimeters for gamma ray detection [12] and blue-light sensors [13–15] was recently demonstrated by some of the authors that uses the radiation stability of the optical properties of tris-(8-hydroxyquinoline)aluminum – Alq_3 in chloroform solution combined with the radiation instability of poly(2-methoxy-5(2′-ethylhexyloxy)-p-phenylenevinylene) – MEH-PPV to yield an optically integrated and multifunctional material. The results presented in these papers demonstrate the potential use of MEH-PPV and MEH-PPV/Alq_3 as smart systems for ionizing and non-ionizing radiation detectors whose cumulative dose is easily indicated by a multicolored change associated with the radiation-induced degradation processes of MEH-PPV. These results reveal, on the one hand, the potential use of a luminescent polymer as an active material for ionizing radiation detectors and, on the other hand, reflect, for the first time, the scope of using the combination of a light-emitting polymer and a metal complex with a difference in optical emission and in their degradation rates induced by radiation to form a potential hybrid system which are rarely seen together. In view of the growing interest in improving patient safety in radiation oncology [8,9], it thus appears promising to use this hybrid system as active material for high energy X-ray detectors. The initial motivation for this work on the evaluation of a high-energy X-ray dose radiation detector was to attempt to develop a smart, easy-to-read, and inexpensive reference radiation monitoring organic device based on the substantial dependence of the optical properties of MEH-PPV/Alq_3 on X-ray dose. This device is thus capable of recording the total dose delivered to the oncology patient shortly before a LINAC-based treatment.

2. Experimental procedures

Poly (2-methoxy-5(2′-ethylhexyloxy)-p-phenylenevinylene) – MEH-PPV and tris-(8-hydroxyquinoline)aluminum – Alq_3 were purchased from Sigma Aldrich and dissolved in chloroform at MEH-PPV/Alq_3 wt/wt solutions equal to 1/2 as described elsewhere [13]. The solutions were transferred to glass ampoules which were then flame-sealed to avoid solvent evaporation. The specifications for the ampoules are as follows: nominal volume, diameter, external thickness and wall thickness of 1.25 ml, 10 mm, 8.0 mm and 0.50 mm, respectively. The irradiation of the samples by X-rays was performed in the dark at the Radiotherapy Center of Cristiano Varella Foundation, Brazil to evaluate the effect of ionizing radiation in the range of 0–40 Gy on the optical properties of MEH-PPV/Alq_3 hybrid material. In the present study, Varian Clinac 600C LINAC computer-controlled equipment with a conventional X-ray source was used. This machine generates a 6 MV X-ray beam with rectangular symmetric fields [11] and delivers the exact prescribed dose to the patient in the lowest number of monitoring units. The irradiation of samples was performed in a water phantom according to IAEA TRS 398 dosimetry protocols [16] at a source-surface distance of 100 cm with a (30×30) cm^2 field in order to maintain the chief conditions of cancer treatment. Computer tomography of the organic systems was also performed by using the same Varian Clinac 600C LINAC to obtain the physical dose parameters describing the dose distribution in the target samples. The photoemission (PL) spectra of MEH-PPV/Alq_3 systems were recorded using an USB2000 Ocean Optics spectrophotometer, while an InGaN laser (405 nm, 5 mW) was used as the excitation source. Finally, UV–vis absorption spectra were carried out in the 300–800 nm range using the Shimadzu UV 1650 equipment, and the color coordinates of CIE
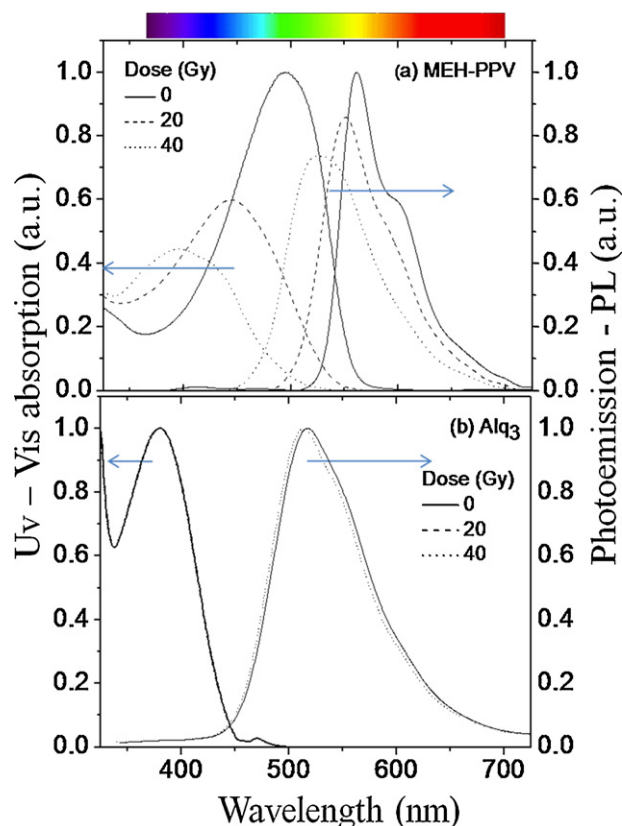

Fig. 1. UV–vis absorption and photoemission (PL) spectra obtained from (a) MEH-PPV and (b) Alq_3 solutions exposed to 0, 20 and 40 Gy of high energy X-rays (6 MV). The visible electromagnetic spectrum shown on top of the graphic is intended to guide the eyes and shows the color-changing of MEH-PPV induced by radiation. (For interpretation of the references to color in the text, the reader is referred to the web version of the article.)

(1931) chromaticity diagram were obtained using the PL spectra of organic solutions and the Color Calculator Free software from Radiant Imaging. All measurements were performed at room temperature.

3. Experimental results

Fig. 1 displays the effect of radiation dose (0, 20 and 40 Gy) delivered by LINAC on the variation of UV–vis absorption and photoemission (PL) properties of MEH-PPV (Fig. 1a) and Alq_3 (Fig. 1b) solutions. It should be noted that dose changes have larger and irreversible effects on the optical properties of MEH-PPV, but have little effect on the same properties of Alq_3. It can be seen from these results that increased dose radiation results in the UV–vis absorption and PL peaks of MEH-PPV shifting towards lower wavelengths and decreasing in intensity, while the UV–vis absorption and PL peaks of Alq_3 are slightly altered by the radiation. As suggested by the previous work of some of the authors on the effect of ionizing and non-ionizing radiation of conjugated polymers [12–15,17], we assume that the blue shift in the UV–vis absorption and PL peak positions of MEH-PPV result from the decrease of the effective conjugation length, and perhaps also from the free radical formed as the primary products during $CHCl_3$ degradation caused by ionizing radiation exposure [18]. Since most free radicals are very reactive and have a short lifetime, they can suffer an acceleration of several steps in the degradation process of MEH-PPV induced by the irradiation process, but do not influence the optical properties of Alq_3. In order to confirm the second assumption, the use of other solvents, such as toluene, instead of chlorinated-solvents is underway
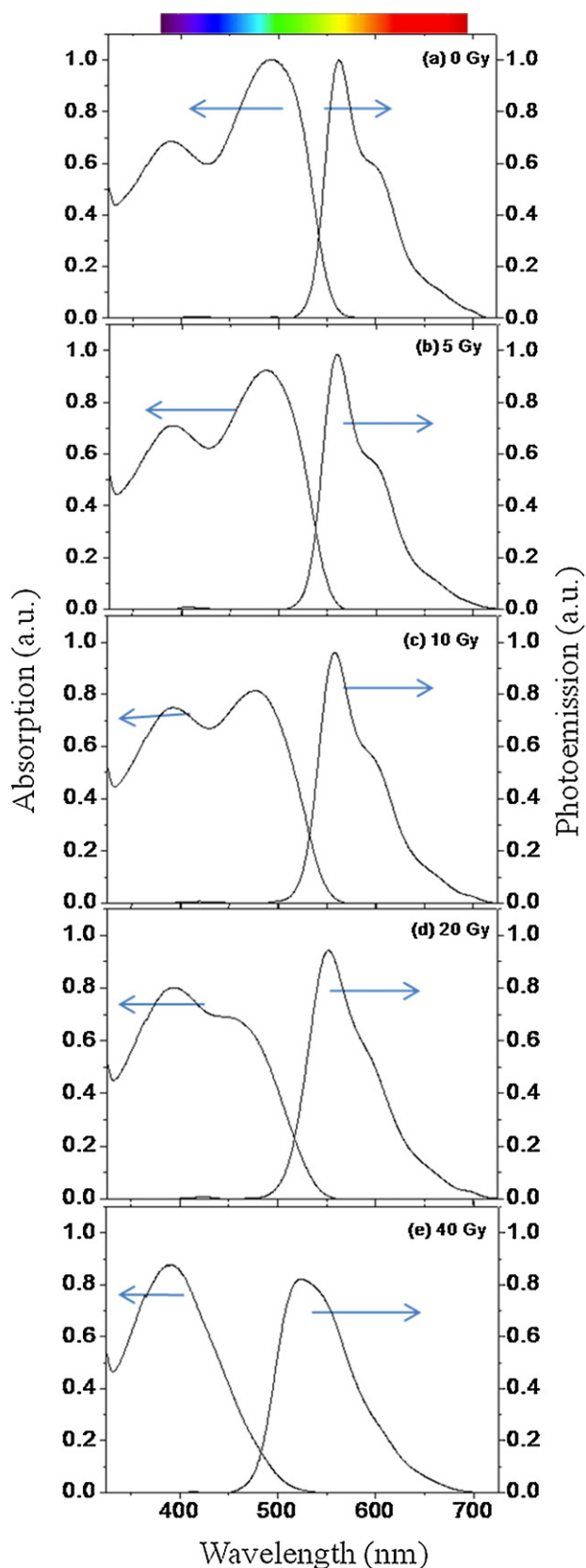
Fig. 2. UV–vis absorption and PL spectra obtained from MEH-PPV/Alq$_3$ hybrid material after exposure to doses of 0, 2.5, 5.0, 7.5, 10.0, 12.5, 15.0, 20.0 and 40 Gy. The visible electromagnetic spectrum shown on top of the graphic is intended to guide the eyes and shows the blue-shift in UV–vis absorption and PL spectra of MEH-PPV/Alq$_3$ induced by radiation. (For interpretation of the references to color in this figure legend, the reader is referred to the web version of the article.)
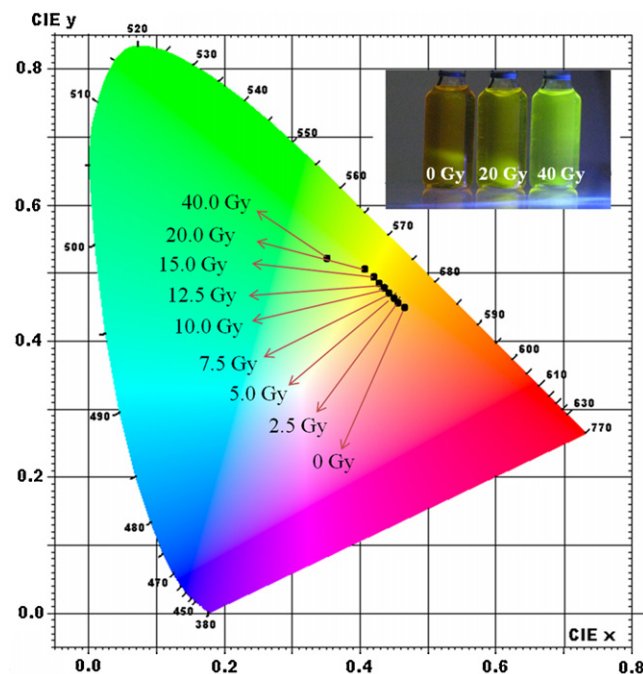

Fig. 3. Chromatic diagram of MEH-PPV/Alq$_3$ chloroform solutions after exposure to doses of 0, 2.5, 5.0, 7.5, 10.0, 12.5, 15.0, 20.0 and 40 Gy. The right-top picture shows red, yellow and green MEH-PPV/Alq$_3$ solutions after exposure to doses of 0, 20 and 40 Gy, respectively. (For interpretation of the references to color in this figure legend, the reader is referred to the web version of the article.)

[18]. However, the foregoing arguments, although in favor of how the optical properties of MEH-PPV are affected by radiation, alone cannot explain the mechanisms involved in the color change of MEH-PPV in CHCl$_3$ during the radiation process, and thus it is speculated here that Cl radicals can be formed during irradiation and react with the polymer leading to a decrease in the effective conjugation length of MEH-PPV [18]. Here it is established that CHCl$_2^\bullet$ and Cl$^\bullet$ are products of CHCl$_3$ exposed to radiation. These radicals can initiate oxidation reactions in the polymeric chain of MEH-PPV. Since the optical spectra of Alq$_3$ were not shifted with the radiation exposure, we assume that the radiation and the presence of radicals did not cause changes in the molecule. The chemical reactions in the MEH-PPV chain and Alq$_3$ molecule will be explained in future work by the NMR and FTIR spectroscopies and GPC chromatography [18].

The phenomenon of multicolored MEH-PPV shown in Fig. 1a has not only revealed the irreversible changes of MEH-PPV from red to light yellow that occur during the radiation process, but also provided a sensitive and convenient probe for monitoring and evaluating the radiation dose in the range of 0–40 Gy. Moreover, a spectral overlap of the Alq$_3$ green emission (Fig. 1b) with the pristine and radiation damaged MEH-PPV absorption (Fig. 1a) is observed. As dose increases, the overlapping gradually tends towards zero. The MEH-PPV degradation and the Alq$_3$ stability under irradiation are the key to develop an irreversible color-change from red to yellow, and then to green, in organic radiation detector.

In Fig. 2 it is displayed the effect of X-ray radiation on the optical properties of MEH-PPV/Alq$_3$ system. Special care was taken to see whether the Alq$_3$ and X-ray played any part in the changes in the UV–vis absorption and PL spectra of the hybrid material.

There is a common pattern in Figs. 1 and 2. Considering the initial optical properties of MEH-PPV/Alq$_3$, it is possible to distinguish between the contributions of MEH-PPV (Fig. 1a) and Alq$_3$ (Fig. 1b) in the pronounced spectral overlap observed in the UV–vis absorption and PL spectra of the hybrid material (Fig. 2a). In addition, the
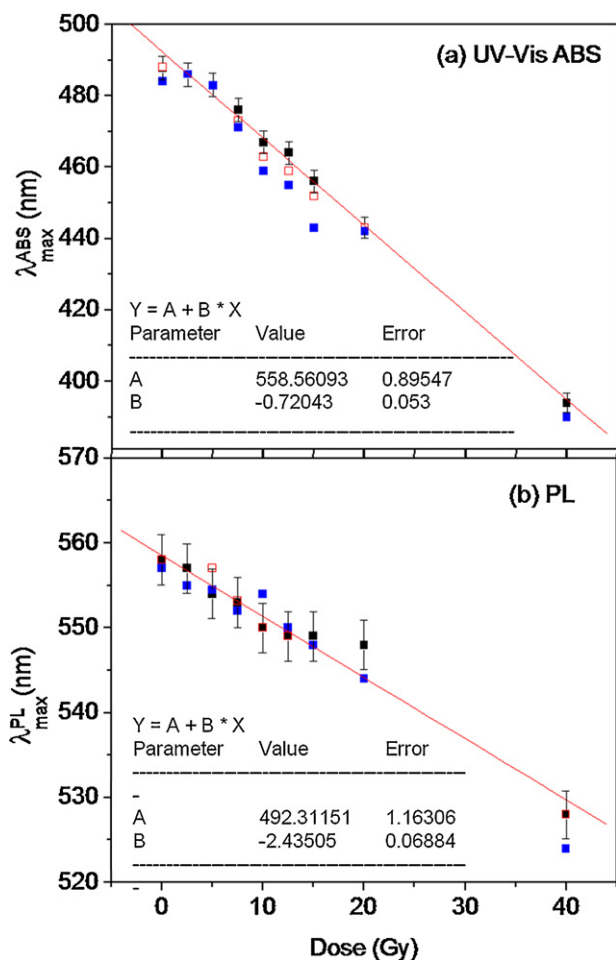
Fig. 4. Wavelengths of the most intense UV–vis absorption (λ_{max}^{ABS}) and PL (λ_{max}^{PL}) of MEH-PPV/Alq$_3$ chloroform solutions obtained from the spectra of Fig. 2 as a function of the radiation dose. The full lines denote the linear regression lines.

optical characteristics of pristine MEH-PPV/Alq$_3$ (Fig. 2a) are not related (at least, directly) to the variations of chemical structure of MEH-PPV and Alq$_3$. However, the major features to notice in Fig. 2a–e are the progressive ionizing radiation-induced degradation of MEH-PPV which leads to emission color of MEH-PPV/Alq$_3$ tuning from red to green with the increase in radiation dose. This is also illustrated by the pictures and in the chromaticity diagrams of pristine and irradiated hybrid material shown in Fig. 3, and it is clear from this evidence that color was used to guide the search for a color-indicator dosimeter. Moreover, the UV–vis absorption and PL spectra of the MEH-PPV/Alq$_3$ after exposure to doses of 40 Gy (Fig. 2e) are the same of Alq$_3$ with one emission peak at around 380 nm and 515 nm (Fig. 1b), respectively. Finally, the color change of the hybrid material is consistent with the replacement of the vinyl group by carbonyl groups on the MEH-PPV backbone [17,19,20] mainly because of degradation processes induced by X-rays. It reduces the average effective polymer conjugation length and usually acts as a quenching center for excitonic emission.

Real time monitoring dosimeters require fast and precise operation. One observation, which follows regardless of the choice of color-change of the hybrid material, is that the tuning from red to any color, shown on the CIE chromatic diagram (Fig. 3), that occurs during the irradiation process is irreversible and the final color is stable for at least three months when the organic solutions are stored in the dark at room temperature. Our task now is to identify the linearity and sensitivity of the sensor response. First of all, we restricted consideration to the set of 27 ampoules filled with
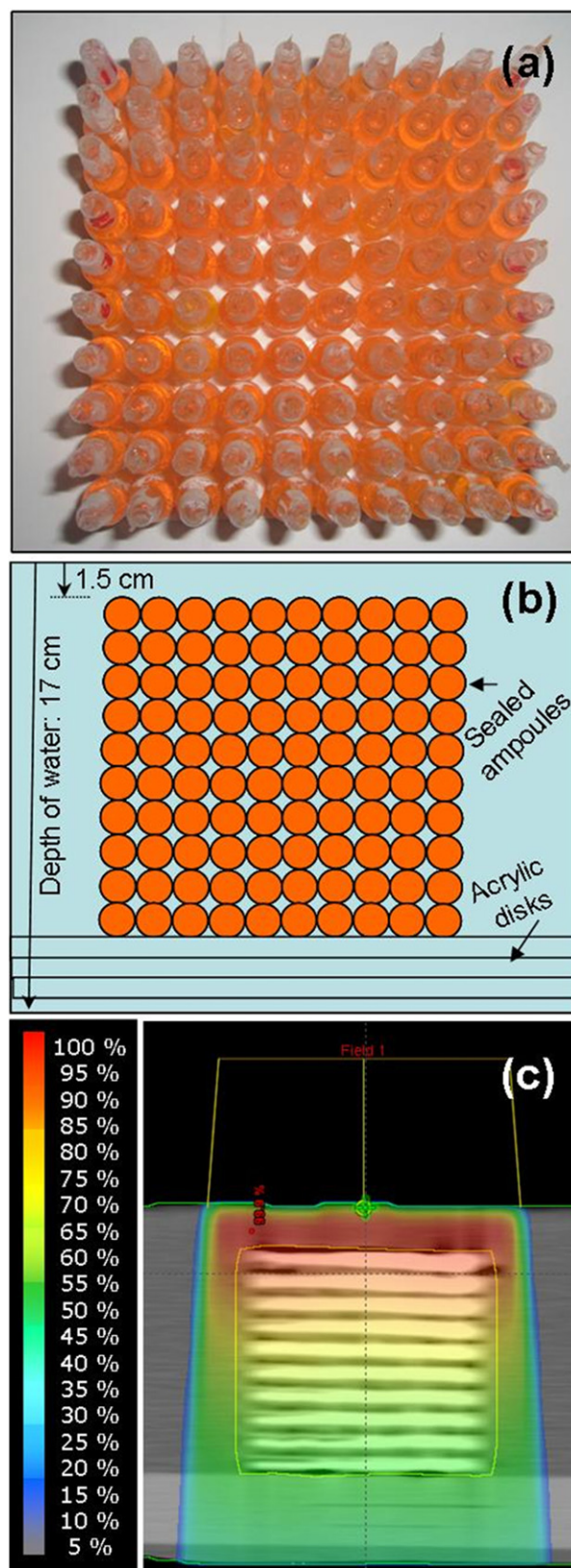

Fig. 5. (a) Set of 10 × 10 sealed glass ampoules filled with MEH-PPV/Alq$_3$ chloroform solutions. (b) Schematic representation of the setup used in the depth-dose simulations. (c) Computed tomographic image of the location of the ampoules (isodose analysis).
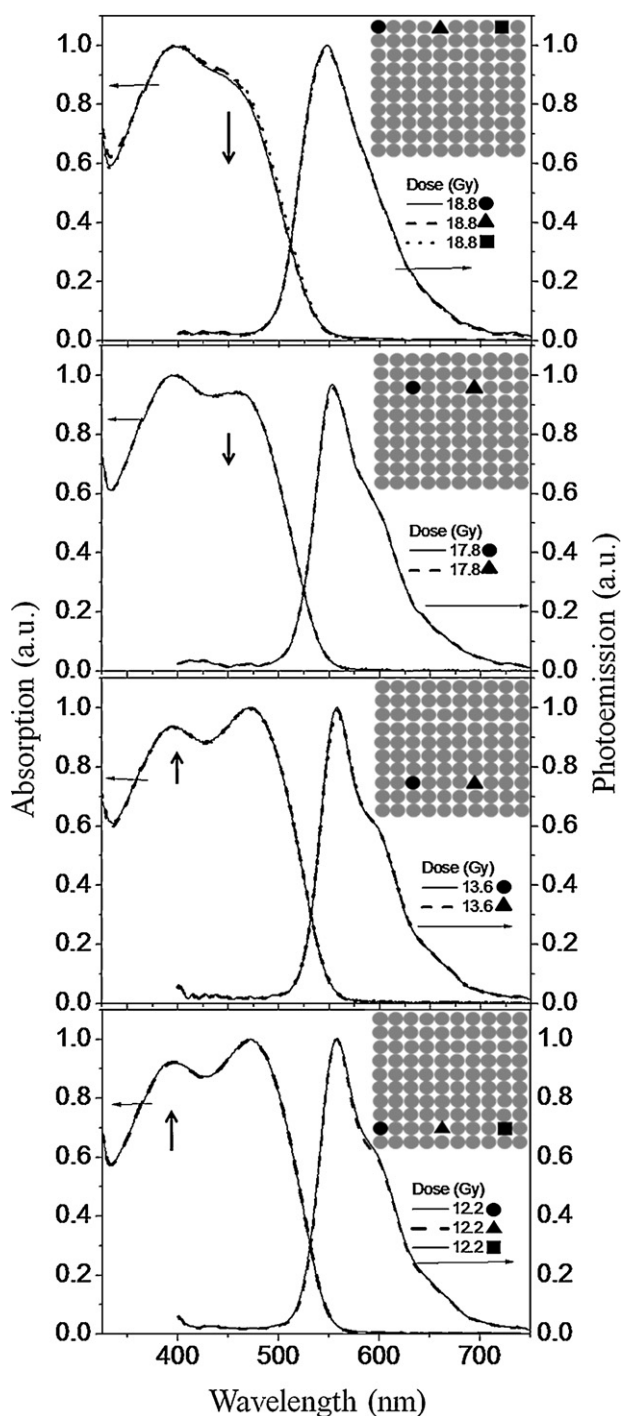
Fig. 6. Sealed glass ampoules filled with MEH-PPV/Alq$_3$ chloroform solutions arranged along the *x*-axes and after exposure to doses of 18.8 Gy, 17.8 Gy, 13.6 Gy and 12.2 Gy. The top right picture shows the quadratic arrangement identified with analyzed (black circles, black squares and black triangles) and non-analyzed (gray circles) samples. Dose values were determined by using the isodoses shown in Fig. 5c.

Fig. 7. Sealed glass ampoules filled with MEH-PPV/Alq$_3$ chloroform solutions arranged along the *y*-axes and after exposure to doses of 18.8, 17.0 Gy, 15.2 Gy, 13.6 Gy and 12.2 Gy. The top right picture shows the quadratic arrangement identified with analyzed (black circles, black squares and black triangles) and non-analyzed (gray circles) samples. Dose values were determined by using the isodoses shown in Fig. 5c.

pristine MEH-PPV/Alq$_3$ solution following the procedure described in Section 2. From this set of ampoules, all three of them were irradiated with the same dose (0, 2.5, 5.0, 7.5, 10.0, 12.5, 15.0, 20.0 or 40.0 Gy). This procedure achieves reasonable agreement with experimental results shown in Fig. 2 (and therefore they are not shown in this paper), guaranteed reproducibility in the preparation process, and also the high optical performance of the organic solution.
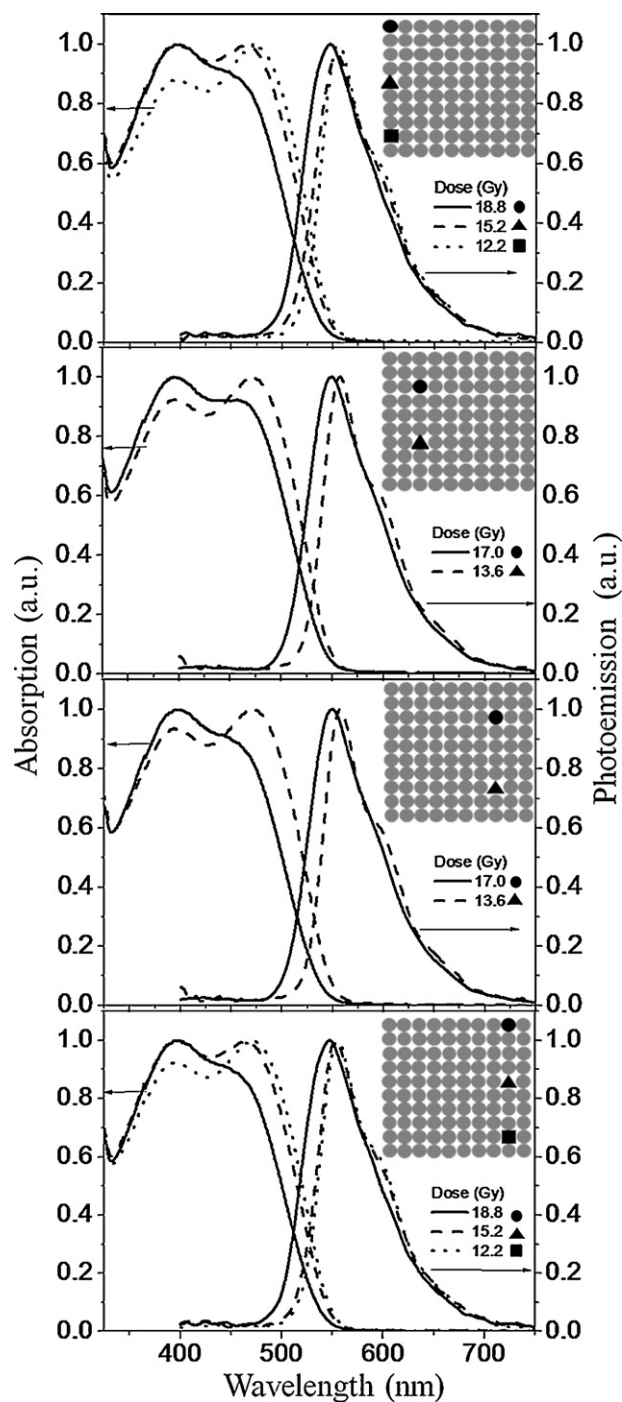
In order to obtain the linearity of the sensor response, we considered the wavelengths of the most intense UV–vis absorption (λ_{max}^{ABS}) and PL (λ_{max}^{PL}) spectra, but reasonably practical parameters, in Fig. 3. Fig. 4 shows the linear radiation-dose dependence of λ_{max}^{ABS} and λ_{max}^{PL}, and also the linear regression of λ_{max}^{ABS} and λ_{max}^{PL} on dose (full lines). It a lowest percentage error is obtained somewhere around 1% and a larger linearity covering a wide range of characteristic radiation dose available at Radiotherapy Centers.
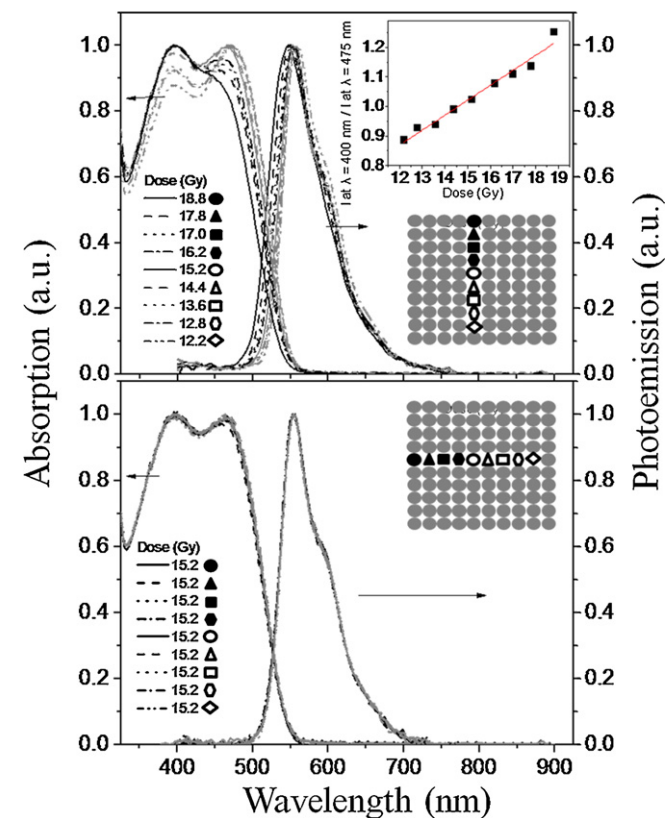
Fig. 8. Sealed glass ampoules filled with MEH-PPV/Alq$_3$ chloroform solutions arranged (a) along the *y*-axes after exposure to doses ranging from 12.2 to 18.8 Gy, and (b) along the *x*-axes after exposure to 15.2 Gy. The right pictures on these graphics show the quadratic arrangement (Fig. 5b) identified with analyzed (black circles, black squares and black triangles) and non-analyzed (gray circles) samples. Dose values were determined by using the isodoses shown in Fig. 5c. The inset figure shows the linear radiation-dose dependence of the relation between the absorption intensities at 400 nm and at 475 nm.

In order to determine the sensitivity of the sensor response, 100 sealed glass ampoules filled with pristine MEH-PPV/Alq$_3$ solutions placed in a quadratic arrangement (10×10 ampoules) were exposed to X-rays in a water phantom for determination of the dynamic beam isodose. Bearing these points in mind, we found that the design procedure requires straightforward depth-dose simulation with Computed Tomographic (CT) images of the ampoules inside the water phantom (isodose analysis).

Fig. 5 shows the quadratic arrangement (Fig. 5a), the schematic representation of the setup used in the depth-dose simulations (Fig. 5b), and the CT image of ampoules (Fig. 5c). Straightforward calculations show unavoidable practical imperfections in the isodose determination for each ampoule due to the large diameter of this system ($= 10$ mm) if compared to the depth-dose variation in the same scale. Thus, it may introduce a new source of error in the induced-radiation effect on the optical properties of MEH-PPV/Alq$_3$. In consequence, we assumed that the organic solution will receive an average dose per ampoule, which is proportional to the isodose calculated at the central axis of the ampoules.

Figs. 6–8 show the UV–vis and PL spectra of several samples exposed to X-ray as shown in the schematic representation of Fig. 5b. The inset in these figures show the relative position between the ampoules filled with the MEH-PPV/Alq$_3$ (dark circles, triangles and squares) used to track the progress on the optical properties of the hybrid material induced by different radiation doses. The quadratic arrangement was found to be very useful for investigating isodoses on water phantoms, since the organic solutions exposed to an isodose curve (along the *x*-axis, Figs. 6 and 8a) show

similar UV–vis and PL curves, while those distributed along different isodoses (along *y*-axis, Figs. 7 and 8b) show considerable change that emphasizes that the variations of these curves are more pronounced the higher the difference between the isodoses is. Nevertheless, if one estimates an average of isodoses from the proposed method, the values between the doses on the top and on the bottom of a quadratic arrangement of organic solutions are easily obtained.

4. Conclusions

MEH-PPV/Alq$_3$ is a suitable smart material for application in a novel, disposable, and personal real-time radiation sensor to avoid hazardous situations. The overlap between the emission spectrum of Alq$_3$ and the absorption spectrum of pristine and damaged MEH-PPV is the operating principle of this sensor which works as a novel "*traffic light device*". A series of experiments was performed, demonstrating linearity in the shift of PL and absorption as a function of the dose. It is also shown therefore that an array of vials containing solutions can be used to map the 2D radiation dose delivered in a water-based phantom. What makes this an outstanding device is the easy indication of the delivered radiation dose to a target material, thus ensuring proper functioning of LINACs. Although each patient is different and therefore each radiotherapy treatment is unique, it is important to remark that the monitoring of this device may also be achieved by first establishing calibration condition values obtained by passing a specific delivered radiation dose to the MEH-PPV/Alq$_3$ system with different composition (wt/wt). This innovative tool must be carefully designed to obtain the maximum advantages: a personal, very low cost (<US$ 1), and easy-to-read dose indicator device. These advantages are key requirements for the successful development of innovations in radiation therapy. One of the benefits often pointed out in connection with Ref. [8] is that the X-ray dose detector based on color-changing of MEH-PPV/Alq$_3$ has the capability of easily providing the radiation dose shortly before the radiation treatment of cancer patients, avoiding a fatal overdose. In fact, conventional dosimeters offer an electrical read-out that is significantly easier to monitor than a dosimeter where a spectroscopic measurement is required to determine the delivered dose. However, the idea that each patient will be able to monitor the response of the radiation detector using a standardized color chart shortly before being irradiated with miscalibrated radiotherapy machines ensures that every treatment will be as safe as possible, avoiding any hazard. A check against the organic solution and the color chart easily indicates the dose delivered from the LINAC. A more practical implementation of such technology would clearly need to be based on a solid thin film for a number of safety reasons and to be easily used in clinical applications, and thus becoming an important subject of study for future publications.

References

[1] E.B. Podgorsak, Radiation Physics for Medical Physicists, first ed., Springer, New York, 2005.
[2] M. Goiteing, Radiation Oncology: A Physicist's – Eye View, first ed., Springer, Nova York, 2008.

[3] C.M. Washington, D. Leaver, Principles and Practice of Radiation Therapy, third ed., Mosby, 2009.

[4] B. Mou, A.L. Cooke, K. Suderman, Radiation oncology in a Canadian providence: measurement of workload and treatment complexity, Clin. Oncol. 23 (2011) 4–9.

[5] D. Greene, P.C. Williams, Linear Accelerator for Radiation Therapy, second ed., Taylor & Francis, 1997.

[6] O.S. Abdelaziz, A. Kandil, S. El-Assall, A. Rashed, Linear accelerator-based stereotactic radiosurgery of intracranial meningiomas: results of the first 5 year of clinical practice, Neurosurg. Rev. 34 (2011) 87–89.

[7] P. Biggs, Evidence for a significant timer error on a linear accelerator: consequences for a special therapy application, Phys. Med. Biol. 43 (1998) 3139–3143.

[8] W.R. Hendee, M.G. Herman, Improving patient safety in radiation oncology, Med. Phys. Lett. 38 (1) (2011) 78–82.

[9] S.J. Goetch, Linear accelerator and gamma knife-based stereotactic radiosurgery: challenges and successes of existing quality assurance guidelines and paradigms, Int. J. Radiat. Oncol. Biol. Phys. 71 (2008) 118–121.

[10] W. Bogdanich, Radiation Offers New Cures and New Ways To Do Harm, New York Times, 2010 January 23.

[11] R.V. Souza:, Dose rate influence on deep dose deposition using a 6 MV X-ray beam from a linear accelerator, Braz. J. Phys. 39 (2) (2009) 292–296.

[12] J.F. Borin, E.S. Brito, P. Nicolutti, C.F.O. Graeff, R.F. Bianchi, Low dose ionizing radiation detection using conjugated polymer, Appl. Phys. Lett. 86 (2005) 131902-1–131903-3.

[13] G.R. Ferreira, C.K.B. de Vasconcelos, R.F. Bianchi, Design and characterization of a novel indicator dosimeter for blue-light radiation, Med. Phys. 36 (2009) 642–644.

[14] C.K.B. de Vasconcelos, R.F. Bianchi, A blue-light dosimeter which indicates the dose accumulation by a multicoloured change of photodegraded polymer, Sens. Actators B: Chem. B 143 (2009) 30–34.

[15] G.R. Ferreira, C.K.B. de Vasconcelos, M.M. Silva, F.A. dos Santos, J.G. Pires, A.S. Duarte, A.G.C. Bianchi, R.F. Bianchi, A novel and low-cost disposable device for phototherapy of neonatal jaundice, Mater. Res. Soc. Symp. Proc. 1 (2010), 1209-P03-03–1209-P03-09.

[16] International Atomic Energy Agency, Absorbed Dose Determination in External Beam. Radiotherapy, Technical Reports Series No. 398, IAEA, Vienna, 2000.

[17] R.F. Bianchi, D.T. Balogh, M. Tinani, R.M. Faria, E.A. Irene, Ellipsometry study of the photo-oxidation of poly(2-methoxy-5-hexyloxy-p-phenylenevinylene), J. Polym. Sci. B 42 (2004) 1033–1041.

[18] G.R. Ferreira, B. Novack, E.R. deAvezedo, L.C. Akcelrud, R.F. Bianchi, Effect of free radicals on the photo-oxidation process in M-PPVs polymers, Mater. Res. Soc. Symp. Proc. 1 (2011) 01–06.

[19] B.H. Cumpston, K.F. Jensen, Photooxidative stability of substituted poly(phenylene vinylene) (PPV) and poly(phenylene acetylene) (PPA), J. Appl. Polym. Sci. 69 (1998) 2451–2458.

[20] B.H. Cumpston, K.F. Jensen, Photooxidation of polymers used in electroluminescent devices, Synth. Met. 73 (3) (1995) 195–199.

Biographies

Thiago Schimitberger is a PhD candidate of Federal University of Minas Gerais in Science and Nuclear Techniques. His current research is the fabrication of X-ray dosimeter and its application in medical fields.

Giovana Ribeiro Ferreira is a PhD candidate of Federal University of Ouro Preto in Materials Science and Engineering. Her current research is the investigation of photodegradation process of poly(p-phenylene vinylenes) derivative.

Marcelo Frota Saraiva received his Medical Physics Specialization degree from Hospital of the Medical School of University of São Paulo. Presently, he is the coordinator of Radiotherapy Center of Cristiano Varella Foundation (Hospital do Câncer de Muriaé), Muriaé Brazil. His main research interests include radiation therapy and medical devices.

Andrea Gomes Campos Bianchi received her PhD degree from University of São Paulo in 2003, and currently she is an affiliate research at Visualization Group at Lawrence Berkeley National Laboratory. She is a Professor in Department of Physics, Federal University of Ouro Preto, MG Brazil.

Rodrigo Fernando Bianchi is a professor in Department of Physics, Federal University of Ouro Preto, MG Brazil. He received his PhD in Materials Science and Engineering from University of São Paulo in 2002. He served as a postdoctoral research associate at the Institute of Physics of São Carlos at University of São Paulo (2002–2006). Presently, he is a vising scholar at Department of Electrical Engineering and Computer Science at University of California - Berkeley, USA. His current research interests include organic electronic and medical devices.